deletion mutants compared with NC-14 cells regardless of the incubation time after cisplatin exposure (Fig. 3D). These results suggested that the decreased intracellular platinum contents were associated with platinum resistance of the cells transfected with ANXA4 full length and each deletion mutant.

The calcium-binding site of the annexin repeat is responsible for platinum resistance

As specified above, platinum resistance was enhanced in cells overexpressing ANXA4 deletion mutants, which contained at least 1 intact annexin repeat. Thus, to assess whether the calcium-binding site of the annexin repeat sequence was involved in chemoresistance, another deletion mutant, R1(E70A) was constructed. Within the annexin repeat next to the N-terminal region, the 70th amino acid, glutamic acid, was responsible for the calcium-dependent activity of ANXA4 [30]. Accordingly, at this site, the point mutation variant of R1, R1(E70A), loses the function of its calcium-binding site (Fig. 4A). Similar to other deletion mutants, R1(E70A) was transfected into NUGC3 cells and designated R1(E70A)-95. Western blotting revealed that R1-12 had the same molecular weight as R1(E70A)-95 (Fig. 4B). R1(E70A)-95 did not induce resistance to either cisplatin or carboplatin (Fig. 4C). Moreover, the intracellular platinum content of R1(E70A)-95-transfected cells did not decrease compared with that of NC-14 cells after 0 hr

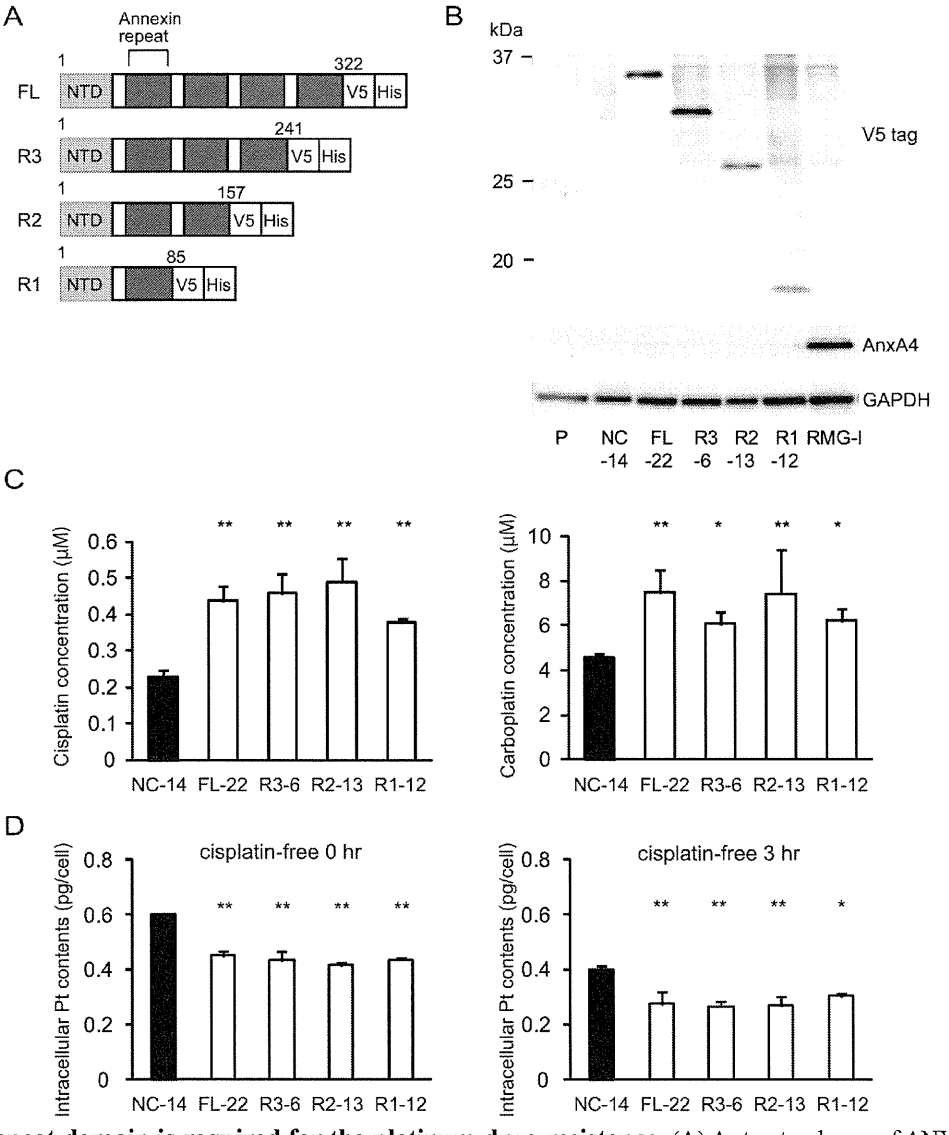

Fig.3: Annexin repeat domain is required for the platinum drug resistance. (A) A structural map of ANXA4 and 3 deletion mutant proteins. Annexin repeats were deleted one by one from the C-terminal site. (B) Established deletion mutant cells together with parent cells, control cells and RMG-I as a positive control were confirmed using Western blotting. (C) Compared with NC-14 cells, IC_{50} for both cisplatin and carboplatin was significantly increased in FL-22 and all other mutant cells. (D) Intracellular platinum accumulation after treatment with 100 μM cisplatin for 60 min with or without additional 3 hr of incubation in cisplatin-free medium. Data are presented as mean ± SD (*$p < 0.05$, **$p < 0.01$).

or 3 hr of additional incubation in cisplatin-free medium (Fig. 4D). According to the above results, the platinum resistance of ANXA4 seemed to be related to the calcium-binding site of the annexin repeat next to the N-terminal domain.

The calcium-binding site of the annexin repeated sequence is required for the resistance to platinum-based drugs *in vivo*

To determine whether the annexin deletion mutants of ANXA4 influenced the sensitivity to cisplatin *in vivo*, we inoculated ICR *nu/nu* mice with NC-14, FL-22, R1-12 or R1(E70A)-95 cells. Mice in each group were randomised into 2 subgroups and received either cisplatin at 3 mg/(kg·d) or PBS *i.p.* once a week for 3 weeks. Cisplatin markedly decreased tumour volume in mice injected with NC-14 and R1(E70A)-95 cells, whereas the treatment effect was relatively smaller in mice injected with FL-22 and R1-12 cells (Fig. 5A). Consistent with the tumour volume, tumour growth was significantly inhibited by cisplatin in mice inoculated with NC-14 (96.5 ± 1.3%) and R1(E70A)-95 cells (87.8 ± 11.4%) compared with those injected with FL-22 (48.5 ± 11.7%) and R1-12 cells (37.7 ± 9.8%; $p < 0.01$; Fig. 5B). These *in vivo* results

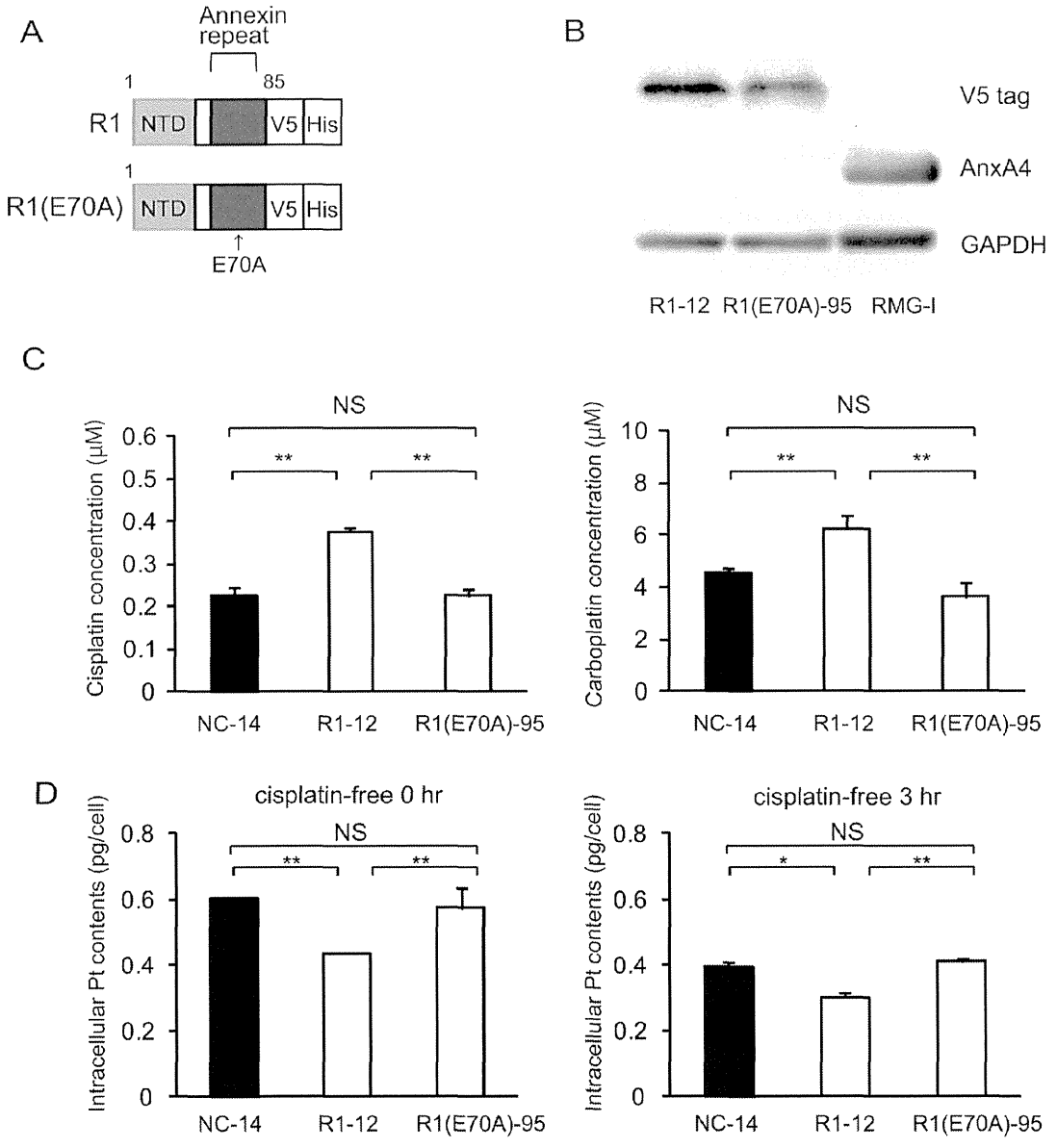

Fig.4: The calcium-binding site of the annexin repeat is responsible for induction of the platinum resistance. (A) A structural map of R1 and R1(E70A) variants without a function for the calcium-binding site. (B) Western blotting confirmed the mutant established cell lines. (C) Unlike R1-12, the R1(E70A)-95 cell clone was not resistant to either cisplatin or carboplatin. (D) Intracellular platinum accumulation in R1(E70A) cells was the same as in NC14 cells both with or without additional 3 hr of incubation in cisplatin-free medium. Data are presented as mean ± SD (*$p < 0.05$, **$p < 0.01$).

were consistent with those obtained *in vitro*.

Increase of the intracellular chloride concentration is related to cisplatin resistance

To elucidate the molecular mechanisms of chemoresistance induced by ANXA4, we focused on the chloride channel because one of the functions of ANXA4 is inhibition of calcium-dependent chloride conductance[32]. According to the literature, treatment with cisplatin induces an increase of the intracellular Ca^{2+} concentration [46], which is an important ion for the phospholipid membrane-binding activity of ANXA4. In contrast, cisplatin exposure also induces an elevation of the intracellular chloride concentration: $[Cl^-]_i$ [47]. Elevation of $[Cl^-]_i$ has been shown to prevent the aquation of 1 or 2 of the 2 chloride coordination sites in cisplatin, and only the aquated forms of cisplatin covalently bind to DNA. Nevertheless, the mechanisms of $[Cl^-]_i$ elevation because of cisplatin treatment have not been fully elucidated. We hypothesised that an increase in intracellular Ca^{2+} concentration after cisplatin exposure would result in translocation of ANXA4 from the cytosol to plasma membrane, which leads to $[Cl^-]_i$ accumulation through inhibition of the chloride channel by the Ca^{2+}-bound ANXA4. To confirm this hypothesis, we quantified $[Cl^-]_i$ after cisplatin treatment using MAQE fluorescence, a fluorescent Cl^- indicator. Relative fluorescence was substituted for $[Cl^-]_i$ as previously reported [48].

We monitored MQAE fluorescence in control cells (NC-14), in cells overexpressing full-length ANXA4 (FL-22) and in 2 deletion mutants (R1-12 and R1[E70A]-95). The relative fluorescence ratio before (F0) and after

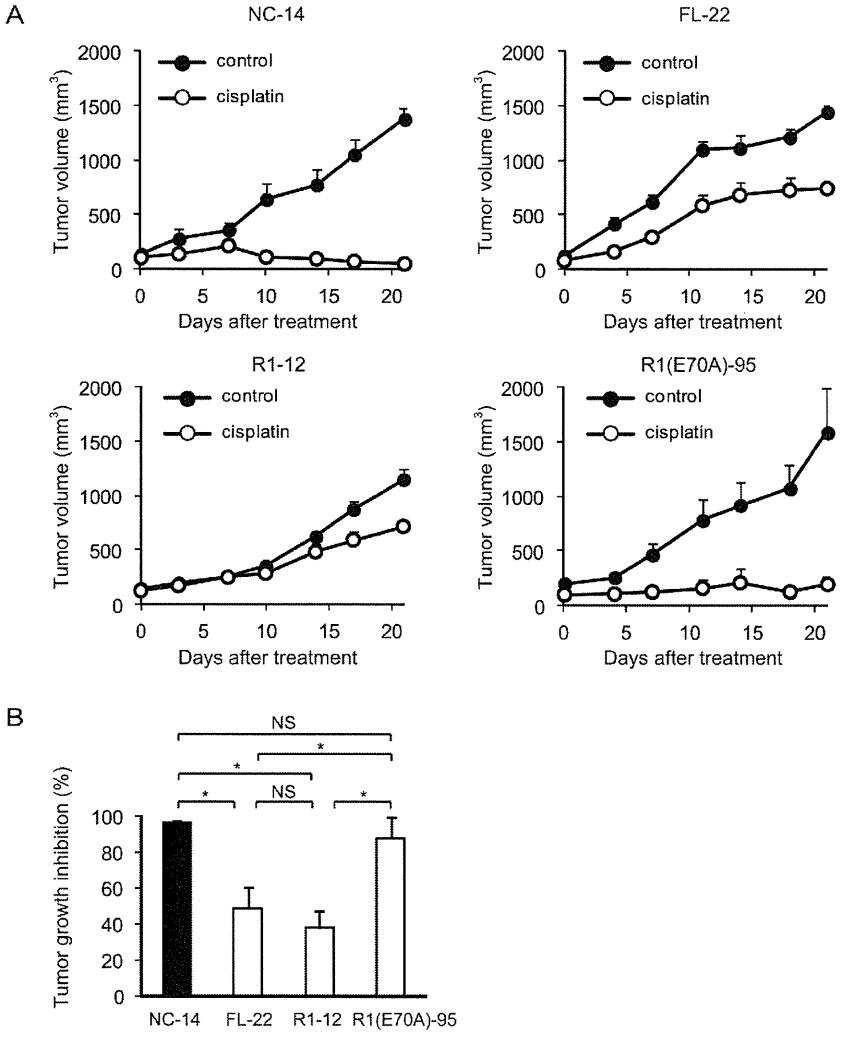

Fig.5: The calcium-binding site of the annexin repeat is required for platinum drug resistance *in vivo*. Female ICR *nu/nu* mice were subcutaneously inoculated with NC14, FL-22, R1-12 or R1(E70A)-95 cells and given PBS (control group: *filled circles*) or cisplatin i.p. (3 mg/kg; treatment group: *open circles*) once a week for 3 weeks (n = 6 per group). (A) Growth curves of tumours of each cell. The mean volume (points) ± SE (bars) is shown. (B) Comparison of the cisplatin-induced growth inhibition of tumours 28 days after treatment. The average (columns) ± SE (bars) are shown; $*p < 0.01$.

treatment with cisplatin for 30 min (F30) is shown in Figure 6. The inverse ratio of MQAE fluorescence 1/(F30/F0), which is directly proportional to the increase in $[Cl^-]_i$, was significantly elevated in the platinum-resistant cell clones FL-22 (1.12 ± 0.03) and R1-12 (1.12 ± 0.01) compared with sensitive clones, NC-14 (1.06 ± 0.01) and R1(E70A)-95 (1.06 ± 0.02; $p < 0.01$). Thus, the increase in $[Cl^-]_i$ is likely to be involved in cisplatin resistance.

DISCUSSION

ANXA4 has been reported to be strongly expressed and involved in chemoresistance in various cancers. The factors associated with ANXA4-induced chemoresistance have been reported, such as NF-κB [45] and ATP7A [44], but the structure of the protein, i.e. annexin repeats and calcium-binding sites in the annexin repeated sequence, has not been taken into account in relation to the ANXA4-induced chemoresistance. In this study, we showed that ANXA4 knockdown improved sensitivity to platinum drugs, and annexin repeats were involved in chemoresistance.

We first confirmed ANXA4 expression in various ovarian adenocarcinoma cell lines. As previously reported [28, 49], ANXA4 is significantly upregulated in clear cell carcinoma cell lines (OVTOKO, OVISE and RMG-I) compared with other histological types (serous and mucinous adenocarcinoma cell lines: A2780, OVCAR3, OVSAHO and MCAS). It has been previously demonstrated that enhanced ANXA4 expression induces platinum resistance both *in vitro* and *in vivo* [28, 44], but whether ANXA4 knockdown attenuates platinum resistance has been unknown thus far. Mogami et al. recently reported that an ANXA4 knockdown improves sensitivity to carboplatin *in vitro* using 2 cell lines of ovarian clear cell carcinoma, OVTOKO and OVISE. To the best of our knowledge, ours is the first study to show that ANXA4 knockdown markedly improves the sensitivity to platinum-based drugs not only *in vitro* but also *in vivo* (Figs. 1 and 2).

The result that ANXA4 knockdown improves sensitivity to platinum-based drugs suggests that ANXA4 is a good therapeutic target. To identify the functional domain(s) of ANXA4 that could be a promising therapeutic target, we focused on annexin repeats and constructed 4 deletion mutants (R3, R2, R1 and R1[E70A]). Resistance to platinum drugs was enhanced in cells transfected with mutants possessing at least 1 intact annexin repeat. In contrast, the sensitivity to platinum-based drugs improved among the R1(E70A)-transfected clones because in those cells, the calcium-binding site did not function properly (Figs. 3C and 4C). This result implies that the ANXA4-induced chemoresistance to platinum-based agents is calcium dependent. It has been reported that cisplatin induced increase of intracellular calcium concentration in chemosensitive cells, but not in resistant cells [46, 50]. Together with this and the data by Chan et al., elevation of intracellular calcium concentration induced by cisplatin treatment may translocate Ca^{2+} bound form of ANXA4 from cytosol to plasma membrane, which results in platinum-resistance[32]. We are currently investigating on further analysis.

By analysing the intracellular platinum accumulation, we attempted to elucidate the mechanism of the platinum resistance induced by ANXA4 and its deletion mutants. When intracellular platinum contents were quantitated just after exposure to cisplatin or 3 hr incubation with cisplatin-free medium after exposure to cisplatin, significantly less platinum accumulated in cells transfected with the full-length ANXA4 (FL-22) and 3 deletion mutants (R3-6, R2-13 and R1-12), all of which enhanced the resistance to the platinum-based drugs. In contrast, R1(E70A)-transfected cells (R1[E70A]-95), which did not induce chemoresistance, had the same amount of platinum accumulation as the control cells (Figs. 3D and 4D). These results suggest that the resistance to the platinum-based drugs is mediated by the decrease in intracellular platinum accumulation, which is calcium dependent. The annexin repeats, especially their calcium-binding sites, may be involved in inhibition of the influx, promotion of the efflux or both of platinum drugs. Recently, Cu transporters (CTR1 for the uptake and ATP7A and ATP7B for the efflux) have been reported to be involved in resistance to both cisplatin and carboplatin [14, 44, 51]. In addition, ANXA4 likely enhance platinum efflux through the interaction with ATP7A [44]. The possible mechanisms of inhibition of the influx mediated by ANXA4 remains unclear and further analyses are needed.

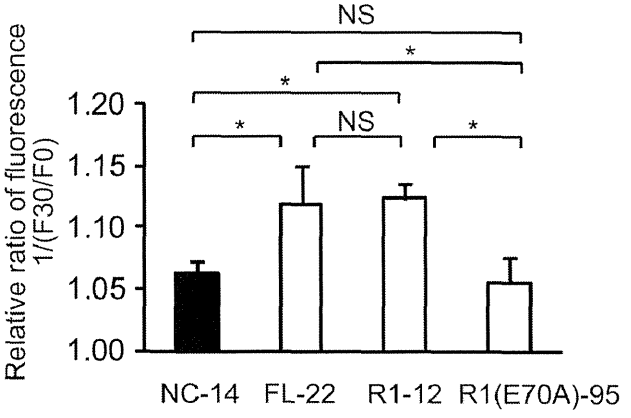

Fig.6: The increase of intracellular chloride concentration is related to cisplatin resistance. ANXA4 deletion mutant series cells (NC-14, FL-22, R1-12 and R1[E70A]-95) loaded with N-ethroxycarbonymethyl-6-methoxyquinolinium bromide (MQAE) were exposed to 100 μM cisplatin. The fluorescence pre-treatment and during treatment (30 min exposure) was compared in each cell clone. Data are presented as mean ± SD (*$p < 0.01$).

Subsequently, the question regarding the involvement of calcium-binding site in the platinum resistance arose. To answer this question, we measured $[Cl^-]_i$ after cisplatin exposure. The significant increase in $[Cl^-]_i$ was observed in the cells with platinum resistance, FL-22 and R1-12, compared with cell clones without platinum resistance, NC-14 and R1(E70A)-95. In a previous study, higher $[Cl^-]_i$ was observed in cisplatin-resistant cells compared with sensitive cells, whereas the intracellular cisplatin accumulation showed the opposite pattern [47]. These results, in addition to the results of decreased platinum accumulation in resistant mutants, indicate that ANXA4 induces platinum resistance through cellular drug efflux partly by elevating the intracellular chloride concentration. We report 'partly' because only cisplatin, not carboplatin, was tested in our $[Cl^-]_i$ assay. Cisplatin becomes intracellularly activated by the aquation of 1 or 2 of the 2 chloride coordination sites, but carboplatin does not contain any chloride coordination sites [1, 52-54]. Thus, this mechanism of resistance through elevation of $[Cl^-]_i$ may be specific to cisplatin and may not be true of carboplatin resistance. In this study, 3 cell clones overexpressing a deletion mutant (R3-6, R2-13, and R1-12) show stronger tolerance to cisplatin than to carboplatin in terms of their IC_{50}; a 1.7- to 2.2-fold increase for cisplatin and only a 1.4- to 1.7-fold increase for carboplatin (Fig. 3C). It is assumed that the increase in $[Cl^-]_i$ is one of the factors inducing cisplatin resistance.

In this study, the calcium-binding site in the annexin repeat next to the N terminus was observed to be responsible for the resistance to the platinum drugs. Nevertheless, the role of the other 3 calcium-binding sites has not yet been investigated. The roles of individual calcium-binding sites were demonstrated using site-directed mutagenesis by Nelson and Creutz regarding calcium-dependent membrane binding and aggregation [30]. The mutations in each domain had different effects on the binding or aggregating activities, i.e. a mutation in the first or fourth domain had a greater effect on membrane binding. A mutation in the second domain had a stronger effect on membrane aggregation, whereas the mutation of the third domain was almost silent. Although the mechanisms involved in membrane binding/aggregation and the mechanisms of chemoresistance are likely different, our data could provide some clues to understanding the function of each annexin repeat and each calcium-binding site in chemoresistance.

ANXA4 has been shown to induce resistance to paclitaxel and platinum-based drugs [55]. The effect of ANXA4 knockdown on paclitaxel sensitivity was assessed in a previous study. The effect of sensitivity to paclitaxel varied among different cell clones: ANXA4 knockdown in the OVTOKO cell line with acidic isoelectric point (IEPs) did not improve the sensitivity to paclitaxel, whereas OVISE cell lines with basic IEPs showed improved sensitivity to paclitaxel [43]. In our own preliminary data, significant chemosensitisation to paclitaxel and etoposide was confirmed in RMG-I Y4 and R5 (data not shown). Further studies are required to identify the detailed mechanism.

In summary, in this study, we observed the annexin repeat, especially its calcium binding site, was associated with platinum-resistance induced by ANXA4, and it happened in calcium-dependent manner. Our findings may help to understand the mechanisms of platinum resistance induced by other annexin family proteins, which possesses the same annexin repeat structure, and offer new strategies for the treatment of chemoresistant cancers.

METHODS

Cell lines and culture

The human ovarian serous adenocarcinoma cell line (OVSAHO), human ovarian mucinous adenocarcinoma cell line (MCAS), human ovarian clear cell carcinoma cell lines (OVTOKO, OVISE and RMG-I) and human gastric cancer cell line (NUGC3) were obtained from the Japanese Collection of Research Bioresources (Osaka, Japan). A2780 cells from the human ovarian serous adenocarcinoma were obtained from the European Collection of Animal Cell Culture (Salisbury, Scotland) and OVCAR-3 cells from another human ovarian serous adenocarcinoma were from American Type Culture Collection (Manassas, VA). MCAS cells were maintained in the DMEM medium and the others in the RPMI medium, all supplemented with 10% foetal bovine serum (FBS; Serum Source International, NC, USA) and 1% penicillin–streptomycin (Nacalai Tesque, Kyoto, Japan) at 37°C in a humidified atmosphere with 5% CO_2. All the cell lines were tested and authenticated.

Generation of ANXA4 knockdown cell lines

To generate stable ANXA4 knockdown cell lines, RMG-I cells were transfected with a commercial plasmid vector expressing short heparin RNA (shRNA) that targeted ANXA4 mRNA or a negative control nonspecific shRNA (SuperArray Bioscience Corp., KH06928N; Frederick, MD, USA) using Lipofectamine 2000 (Invitrogen, Carlsbad, CA), according to the manufacturer's instructions. After selection using a culture medium containing geneticin (600 μg/mL; Invitrogen), stable clones were maintained in 250 μg/mL geneticin. Two stable RMG-I-ANXA4 shRNA cell clones were established, designated Y4 and R5 cells. In addition, we transfected the empty vector into the RMG-I cell line using the same procedure to generate control cells, designated NC7.

Construction of ANXA4 deletion mutants and gene transfection

Using pcDNA3.1-ANXA4 as a template, full-length cDNA of ANXA4 was amplified using KOD-plus (Toyobo Co. Led., Osaka, Japan) with the primers forward 5′-TTGACCTAGAGTCATGGCCA-3′, reverse 5′-ATCATCTCCTCCACAGAGAA-3′ and subsequently ligated into the pcDNA3.1/V5-His-TOPO vector in-frame with the C-terminal V5 and 6× His tag. To generate ANXA4 deletion mutants, annexin repeat domains were deleted one by one from the C-terminal site. Three deletion mutants named R3, R2 and R1 were generated and similarly amplified (an Arabic number shows the number of annexin repeat domains). The nucleotide sequences of the forward primers for PCR were the same as those described above for all the deletion mutants, and the reverse primers were as follows: R3 5′-TATAGCCAGCAGAGCATCTT-3′, R2 5-CAGAGACACCAGCACTCGCT-3′ and R1 5′-CATCCCCACAATCACCTGCT-3′. We subsequently set out to generate an R1 mutant (the E70A mutation), whose calcium-binding site does not work because of the change of a negatively charged carboxyl group to a neutral side chain, as previously described [30]. The site-directed mutagenesis was performed using the KOD-Plus-Mutagenesis kit (Toyobo), according to the manufacturer's protocol. These cDNA fragments, including full-length gene, were subsequently inserted between the *Bgl* II and *EcoR* I sites of the pIRES2AcGFP vector (Clontech, Palo Alto, CA). The sequences of all the mutants were confirmed using the ABI PRISM 3100 Genetic Analyser (Applied Biosystems, Foster City, USA).

Full-length ANXA4, each ANXA4 deletion mutant construct and the empty vector were transfected into NUGC3 cells using Lipofectamine 2000 (Invitrogen). Stable transfectants designated FL-12, R3-6, R2-13, R1-12, R1(R70A)-95 and NC-14 were obtained by selection in a medium containing geneticin and were maintained in the same manner described above.

Western blotting

Cells were lysed in RIPA buffer (10 mM Tris–HCl, pH 7.5, 150 mM NaCl, 1% Nonidet P-40, 0.1% sodium deoxycholate, 0.1% SDS, 1× phosphatase inhibitor cocktail (Nacalai Tesque) and 1× protease inhibitor cocktail (Nacalai Tesque)), followed by centrifugation (13,200 rpm, 4°C, 15 min). Soluble proteins in the supernatant were separated using sodium dodecyl sulphate polyacrylamide gel electrophoresis, as described previously [28]. Additional information can be found in the Supporting Information on Material and Methods section.

Measurement of IC_{50} values after treatment with a platinum-based drug

Cells were suspended in the RPMI medium supplemented with 10% FBS, seeded in 96-well plates (1,500/well for the RMG-I series and 2,500 cells/well for ANXA4 deletion mutant series), cultured for 24 h and exposed to various concentrations of cisplatin (0–25 μM; Sigma–Aldrich, St Louis, MO) or carboplatin (0–1000 μM; Sigma–Aldrich) for 72 h. Cellular proliferation was subsequently evaluated using the WST-8 assay, i.e. 2-(2-methyosy-4-nitro-phenyl)-3-(4-nitrophenyl)-5-(2,4-disulfophynel)-2H-tetrazolium monosodium salt assay (Cell Counting Kit-SF; Nacalai Tesque) after treatment. The absorption of WST-8 was measured at a wavelength of 450 nm (reference wavelength: 630 nm) using a Model 680 microplate reader (Bio-Rad Laboratories, Hercules, CA). Absorbance values for the treated samples were expressed as percentages relative to results for untreated controls, and IC_{50} values were calculated.

Measurement of intracellular platinum accumulation

Full-length ANXA4-transfected cells (FL-22), each ANXA4 deletion mutant-transfected cell clone (R3-6, R2-13, R1-12 and R1[E70A]-95), and control cells (NC-14) were cultured up to 80% confluence in 150-mm tissue culture dishes. The cells were then exposed to 100 μM cisplatin for 60 min at 37°C and washed twice with PBS either immediately or after 3 hr of incubation in cisplatin-free RPMI 1640 medium supplemented with 10% FBS. Whole-cell extracts were prepared, and the concentration of intracellular platinum was determined using an Agilent 7500ce inductively coupled plasma mass spectrometer (ICP-MS; Agilent, Santa Clara, CA, USA).

In vivo model of cisplatin resistance

All animal experiments were conducted in accordance with the Institutional Ethical Guidelines for Animal Experimentation of the National Institute of Biomedical Innovation (Osaka, Japan). Female Institute of Cancer Research (ICR) *nu/nu* mice were obtained from Charles River Japan (Yokohama, Japan). Injection of the ANXA4 knockdown cells was performed as follows: ICR *nu/nu* mice at 4 weeks of age were subcutaneously inoculated (into the flank of the mice; n = 6 per group) with 2.5 × 10^6 cells of RMG-I NC7 cells or RMG-I-Y4 cells in the total volume of 100 μL of 1/1 (v/v) PBS/Matrigel (Becton Dickinson, Bedford, MA). Injection of ANXA4 mutant-transfected cells, i.e. mice at 5 weeks of age were inoculated with 10^6 cells of NC-14, FL-22, R1-12 or R1(E70A) in the same manner

as with the ANXA4 knockdown cells. Treatment with cisplatin (3 mg/kg) or PBS *i.p.* was initiated 1 week after inoculation and administered twice weekly for 4 weeks (ANXA4 knockdown cells) and once a week for 3 weeks (ANXA4 mutant-transfected cells). Tumour volumes were determined twice weekly by measuring length (L), width (W) and depth (D) and using the following formula: tumour volume (mm^3) = W × L × D.

$[Cl^-]_i$ measurements

$[Cl^-]_i$ was measured using the fluorescent Cl^- indicator N-ethroxycarbonymethyl-6-methoxyquinolinium bromide (MQAE; Dojindo, Kumamoto, Japan). $[Cl^-]_i$ is detected by the mechanism of diffusion-limited collisional quenching of MQAE fluorescence. MQAE fluorescence intensity inversely correlates with $[Cl^-]_i$. The cells of the ANXA4 deletion mutant series (NC-14, FL-22, R1-12 and R1[E70A]-95) were cultured in 35-mm tissue culture dishes up to 20% confluence and incubated with a medium containing 10 mM MQAE for 4 h at 37°C. After loading, the cells were washed 5 times with Cl^--free buffer and electrically stimulated under a microscope at 37°C in a humidified atmosphere with 5% CO_2. Fluorescence measurements were initiated immediately at the indicated periods using Biozero BZ-9000 (Keyence, Tokyo, Japan) at 510/40 nm excitation and 380/50 nm emission. The fluorescence was quantitated by means of a standardised procedure using a BZ-II Analyser (Keyence), and the data were presented as the reciprocal of the ratio of fluorescence data (F0/F30) to identify possible correlations with the increase in $[Cl^-]_i$.

Statistical analysis

All calculations involved one-way analysis of variance (ANOVA) followed by Dunnett's analysis to evaluate the significance of differences. In all experiments, p value of <0.05 was considered statistically significant.

ACKNOWLEDGEMENTS

We thank Y. Kanazawa and A. Yagi for their secretarial assistance, M. Ako and E. Harada for technical assistance.

There are no conflicts of interest to declare. This study was supported by a Grant-in-Aid from the Program for Promotion of Fundamental Studies in Health Sciences of the National Institute of Biomedical Innovation; a Grant-in-Aid from the Ministry of Health, Labour and Welfare of Japan and Grants-in-Aid for Young Scientists (B) (22791560) from the Japanese Ministry of Education, Science, Culture and Sports

REFERENCES

1. Kelland L. The resurgence of platinum-based cancer chemotherapy. Nat Rev Cancer. 2007; 7(8):573-584.
2. Loriot Y, Mordant P, Deutsch E, Olaussen KA and Soria JC. Are RAS mutations predictive markers of resistance to standard chemotherapy? Nat Rev Clin Oncol. 2009; 6(9):528-534.
3. Alva AS, Matin SF, Lerner SP and Siefker-Radtke AO. Perioperative chemotherapy for upper tract urothelial cancer. Nat Rev Urol. 2012; 9(5):266-273.
4. Bookman MA. First-line chemotherapy in epithelial ovarian cancer. Clin Obstet Gynecol. 2012; 55(1):96-113.
5. Matos CS, de Carvalho AL, Lopes RP and Marques MP. New strategies against prostate cancer--Pt(II)-based chemotherapy. Curr Med Chem. 2012; 19(27):4678-4687.
6. Rossi A, Di Maio M, Chiodini P, Rudd RM, Okamoto H, Skarlos DV, Fruh M, Qian W, Tamura T, Samantas E, Shibata T, Perrone F, Gallo C, Gridelli C, Martelli O and Lee SM. Carboplatin- or cisplatin-based chemotherapy in first-line treatment of small-cell lung cancer: the COCIS meta-analysis of individual patient data. J Clin Oncol. 2012; 30(14):1692-1698.
7. Muggia FM and Los G. Platinum resistance: laboratory findings and clinical implications. Stem Cells. 1993; 11(3):182-193.
8. Jassem J. Chemotherapy of advanced non-small cell lung cancer. Ann Oncol. 1999; 10 Suppl 6:77-82.
9. Perez RP. Cellular and molecular determinants of cisplatin resistance. Eur J Cancer. 1998; 34(10):1535-1542.
10. Fuertes MA, Castilla J, Alonso C and Perez JM. Novel concepts in the development of platinum antitumor drugs. Curr Med Chem Anticancer Agents. 2002; 2(4):539-551.
11. Gonzalez VM, Fuertes MA, Alonso C and Perez JM. Is cisplatin-induced cell death always produced by apoptosis? Mol Pharmacol. 2001; 59(4):657-663.
12. Niedner H, Christen R, Lin X, Kondo A and Howell SB. Identification of genes that mediate sensitivity to cisplatin. Mol Pharmacol. 2001; 60(6):1153-1160.
13. Ishida S, Lee J, Thiele DJ and Herskowitz I. Uptake of the anticancer drug cisplatin mediated by the copper transporter Ctr1 in yeast and mammals. Proc Natl Acad Sci U S A. 2002; 99(22):14298-14302.
14. Safaei R, Holzer AK, Katano K, Samimi G and Howell SB. The role of copper transporters in the development of resistance to Pt drugs. J Inorg Biochem. 2004; 98(10):1607-1613.
15. Katano K, Kondo A, Safaei R, Holzer A, Samimi G, Mishima M, Kuo YM, Rochdi M and Howell SB. Acquisition of resistance to cisplatin is accompanied by changes in the cellular pharmacology of copper. Cancer Res. 2002; 62(22):6559-6565.
16. Samimi G, Varki NM, Wilczynski S, Safaei R, Alberts DS and Howell SB. Increase in expression of the copper

transporter ATP7A during platinum drug-based treatment is associated with poor survival in ovarian cancer patients. Clin Cancer Res. 2003; 9(16 Pt 1):5853-5859.

17. Rabik CA, Maryon EB, Kasza K, Shafer JT, Bartnik CM and Dolan ME. Role of copper transporters in resistance to platinating agents. Cancer Chemother Pharmacol. 2009; 64(1):133-142.
18. Koike K, Kawabe T, Tanaka T, Toh S, Uchiumi T, Wada M, Akiyama S, Ono M and Kuwano M. A canalicular multispecific organic anion transporter (cMOAT) antisense cDNA enhances drug sensitivity in human hepatic cancer cells. Cancer Res. 1997; 57(24):5475-5479.
19. Cui Y, Konig J, Buchholz JK, Spring H, Leier I and Keppler D. Drug resistance and ATP-dependent conjugate transport mediated by the apical multidrug resistance protein, MRP2, permanently expressed in human and canine cells. Mol Pharmacol. 1999; 55(5):929-937.
20. Liedert B, Materna V, Schadendorf D, Thomale J and Lage H. Overexpression of cMOAT (MRP2/ABCC2) is associated with decreased formation of platinum-DNA adducts and decreased G2-arrest in melanoma cells resistant to cisplatin. J Invest Dermatol. 2003; 121(1):172-176.
21. Ban N, Takahashi Y, Takayama T, Kura T, Katahira T, Sakamaki S and Niitsu Y. Transfection of glutathione S-transferase (GST)-pi antisense complementary DNA increases the sensitivity of a colon cancer cell line to adriamycin, cisplatin, melphalan, and etoposide. Cancer Res. 1996; 56(15):3577-3582.
22. Olaussen KA, Dunant A, Fouret P, Brambilla E, Andre F, Haddad V, Taranchon E, Filipits M, Pirker R, Popper HH, Stahel R, Sabatier L, Pignon JP, Tursz T, Le Chevalier T and Soria JC. DNA repair by ERCC1 in non-small-cell lung cancer and cisplatin-based adjuvant chemotherapy. N Engl J Med. 2006; 355(10):983-991.
23. Wang Q, Shi S, He W, Padilla MT, Zhang L, Wang X, Zhang B and Lin Y. Retaining MKP1 expression and attenuating JNK-mediated apoptosis by RIP1 for cisplatin resistance through miR-940 inhibition. Oncotarget. 2014; 5(5):1304-1314.
24. Li H and Yang BB. MicroRNA in drug resistance. Oncoscience. 2014; 1(1):2.
25. Yang H, Kong W, He L, Zhao JJ, O'Donnell JD, Wang J, Wenham RM, Coppola D, Kruk PA, Nicosia SV and Cheng JQ. MicroRNA expression profiling in human ovarian cancer: miR-214 induces cell survival and cisplatin resistance by targeting PTEN. Cancer Res. 2008; 68(2):425-433.
26. Sorrentino A, Liu CG, Addario A, Peschle C, Scambia G and Ferlini C. Role of microRNAs in drug-resistant ovarian cancer cells. Gynecol Oncol. 2008; 111(3):478-486.
27. Perego P, Giarola M, Righetti SC, Supino R, Caserini C, Delia D, Pierotti MA, Miyashita T, Reed JC and Zunino F. Association between cisplatin resistance and mutation of p53 gene and reduced bax expression in ovarian carcinoma cell systems. Cancer Res. 1996; 56(3):556-562.
28. Kim A, Enomoto T, Serada S, Ueda Y, Takahashi T, Ripley B, Miyatake T, Fujita M, Lee CM, Morimoto K, Fujimoto M, Kimura T and Naka T. Enhanced expression of Annexin A4 in clear cell carcinoma of the ovary and its association with chemoresistance to carboplatin. Int J Cancer. 2009; 125(10):2316-2322.
29. Gerke V and Moss SE. Annexins: from structure to function. Physiol Rev. 2002; 82(2):331-371.
30. Nelson MR and Creutz CE. Combinatorial mutagenesis of the four domains of annexin IV: effects on chromaffin granule binding and aggregating activities. Biochemistry. 1995; 34(9):3121-3132.
31. Kaetzel MA, Hazarika P and Dedman JR. Differential tissue expression of three 35-kDa annexin calcium-dependent phospholipid-binding proteins. J Biol Chem. 1989; 264(24):14463-14470.
32. Chan HC, Kaetzel MA, Gotter AL, Dedman JR and Nelson DJ. Annexin IV inhibits calmodulin-dependent protein kinase II-activated chloride conductance. A novel mechanism for ion channel regulation. J Biol Chem. 1994; 269(51):32464-32468.
33. Kaetzel MA, Mo YD, Mealy TR, Campos B, Bergsma-Schutter W, Brisson A, Dedman JR and Seaton BA. Phosphorylation mutants elucidate the mechanism of annexin IV-mediated membrane aggregation. Biochemistry. 2001; 40(13):4192-4199.
34. Dreier R, Schmid KW, Gerke V and Riehemann K. Differential expression of annexins I, II and IV in human tissues: an immunohistochemical study. Histochem Cell Biol. 1998; 110(2):137-148.
35. Wei R, Zhang Y, Shen L, Jiang W, Li C, Zhong M, Xie Y, Yang D, He L and Zhou Q. Comparative proteomic and radiobiological analyses in human lung adenocarcinoma cells. Mol Cell Biochem. 2012; 359(1-2):151-159.
36. Alfonso P, Canamero M, Fernandez-Carbonie F, Nunez A and Casal JI. Proteome analysis of membrane fractions in colorectal carcinomas by using 2D-DIGE saturation labeling. J Proteome Res. 2008; 7(10):4247-4255.
37. Zimmermann U, Balabanov S, Giebel J, Teller S, Junker H, Schmoll D, Protzel C, Scharf C, Kleist B and Walther R. Increased expression and altered location of annexin IV in renal clear cell carcinoma: a possible role in tumour dissemination. Cancer Lett. 2004; 209(1):111-118.
38. Sitek B, Luttges J, Marcus K, Kloppel G, Schmiegel W, Meyer HE, Hahn SA and Stuhler K. Application of fluorescence difference gel electrophoresis saturation labelling for the analysis of microdissected precursor lesions of pancreatic ductal adenocarcinoma. Proteomics. 2005; 5(10):2665-2679.
39. Xin W, Rhodes DR, Ingold C, Chinnaiyan AM and Rubin MA. Dysregulation of the annexin family protein family is associated with prostate cancer progression. Am J Pathol. 2003; 162(1):255-261.

40. Duncan R, Carpenter B, Main LC, Telfer C and Murray GI. Characterisation and protein expression profiling of annexins in colorectal cancer. Br J Cancer. 2008; 98(2):426-433.
41. Yamashita T, Nagano K, Kanasaki S, Maeda Y, Furuya T, Inoue M, Nabeshi H, Yoshikawa T, Yoshioka Y, Itoh N, Abe Y, Kamada H, Tsutsumi Y and Tsunoda S. Annexin A4 is a possible biomarker for cisplatin susceptibility of malignant mesothelioma cells. Biochem Biophys Res Commun. 2012; 421(1):140-144.
42. Choi CH, Sung CO, Kim HJ, Lee YY, Song SY, Song T, Kim J, Kim TJ, Lee JW, Bae DS and Kim BG. Overexpression of annexin A4 is associated with chemoresistance in papillary serous adenocarcinoma of the ovary. Hum Pathol. 2013; 44(6):1017-1023.
43. Mogami T, Yokota N, Asai-Sato M, Yamada R, Koizume S, Sakuma Y, Yoshihara M, Nakamura Y, Takano Y, Hirahara F, Miyagi Y and Miyagi E. Annexin a4 is involved in proliferation, chemo-resistance and migration and invasion in ovarian clear cell adenocarcinoma cells. PLoS One. 2013; 8(11):e80359.
44. Matsuzaki S, Enomoto T, Serada S, Yoshino K, Nagamori S, Morimoto A, Yokoyama T, Kim A, Kimura T, Ueda Y, Fujita M, Fujimoto M, Kanai Y and Naka T. Annexin A4-conferred platinum resistance is mediated by the copper transporter ATP7A. Int J Cancer. 2013.
45. Jeon YJ, Kim DH, Jung H, Chung SJ, Chi SW, Cho S, Lee SC, Park BC, Park SG and Bae KH. Annexin A4 interacts with the NF-kappaB p50 subunit and modulates NF-kappaB transcriptional activity in a Ca2+-dependent manner. Cell Mol Life Sci. 2010; 67(13):2271-2281.
46. Al-Bahlani S, Fraser M, Wong AY, Sayan BS, Bergeron R, Melino G and Tsang BK. P73 regulates cisplatin-induced apoptosis in ovarian cancer cells via a calcium/calpain-dependent mechanism. Oncogene. 2011; 30(41):4219-4230.
47. Salerno M, Yahia D, Dzamitika S, de Vries E, Pereira-Maia E and Garnier-Suillerot A. Impact of intracellular chloride concentration on cisplatin accumulation in sensitive and resistant GLC4 cells. J Biol Inorg Chem. 2009; 14(1):123-132.
48. Chao AC, Dix JA, Sellers MC and Verkman AS. Fluorescence measurement of chloride transport in monolayer cultured cells. Mechanisms of chloride transport in fibroblasts. Biophys J. 1989; 56(6):1071-1081.
49. Masuishi Y, Arakawa N, Kawasaki H, Miyagi E, Hirahara F and Hirano H. Wild-type p53 enhances annexin IV gene expression in ovarian clear cell adenocarcinoma. FEBS J. 2011; 278(9):1470-1483.
50. Splettstoesser F, Florea AM and Busselberg D. IP(3) receptor antagonist, 2-APB, attenuates cisplatin induced Ca2+-influx in HeLa-S3 cells and prevents activation of calpain and induction of apoptosis. Br J Pharmacol. 2007; 151(8):1176-1186.
51. Safaei R. Role of copper transporters in the uptake and efflux of platinum containing drugs. Cancer Lett. 2006; 234(1):34-39.
52. El-Khateeb M, Appleton TG, Charles BG and Gahan LR. Development of HPLC conditions for valid determination of hydrolysis products of cisplatin. J Pharm Sci. 1999; 88(3):319-326.
53. Kelland LR. Preclinical perspectives on platinum resistance. Drugs. 2000; 59 Suppl 4:1-8; discussion 37-38.
54. Siddik ZH. Cisplatin: mode of cytotoxic action and molecular basis of resistance. Oncogene. 2003; 22(47):7265-7279.
55. Gaudio E, Paduano F, Spizzo R, Ngankeu A, Zanesi N, Gaspari M, Ortuso F, Lovat F, Rock J, Hill GA, Kaou M, Cuda G, Aqeilan RI, Alcaro S, Croce CM and Trapasso F. Fhit delocalizes annexin a4 from plasma membrane to cytosol and sensitizes lung cancer cells to Paclitaxel. PLoS One. 2013; 8(11):e78610

Periostin accelerates human malignant melanoma progression by modifying the melanoma microenvironment

Yorihisa Kotobuki[1,2,a], Lingli Yang[1,a], Satoshi Serada[2], Atsushi Tanemura[1], Fei Yang[1], Shintaro Nomura[3], Akira Kudo[4], Kenji Izuhara[5], Hiroyuki Murota[1], Minoru Fujimoto[2], Ichiro Katayama[1] and Tetsuji Naka[2]

1 Department of Dermatology, Osaka University Graduate School of Medicine, Suita, Japan **2** Laboratory for Immune Signal, National Institute of Biomedical Innovation, Ibaraki, Japan **3** Department of Animal Bioscience, Nagahama Institute of Bio-Science and Technology, Nagahama, Japan **4** Department of Biological Information, Tokyo Institute of Technology, Yokohama, Japan **5** Division of Medical Biochemistry, Department of Biomolecular Sciences, Saga Medical School, Saga, Japan

CORRESPONDENCE Atsushi Tanemura, e-mail: tanemura@derma.med.osaka-u.ac.jp

[a]These two authors contributed equally to this work.

KEYWORDS periostin/malignant melanoma/tumor microenvironment

PUBLICATION DATA Received 29 May 2013, revised and accepted for publication 24 March 2014, published online 26 March 2014

doi: 10.1111/pcmr.12245

Summary

Given no reliable therapy for advanced malignant melanoma, it is important to elucidate the molecular mechanisms underlying the disease progression. Using a quantitative proteomics approach, the 'isobaric tags for relative and absolute quantitation (iTRAQ)' method, we identified that the extracellular matrix protein, periostin (POSTN), was highly expressed in invasive melanoma compared with normal skin. An immunohistochemical analysis showed that POSTN was expressed in all invasive melanoma (n = 20) and metastatic lymph node (n = 5) tissue samples, notably restricted in their stroma. In terms of the intercellular regulation of POSTN, we found that there was upregulation of POSTN when melanoma cells and normal human dermal fibroblasts (NHDFs) were cocultured, with restricted expression of TGF-β1 and TGF-β3. In a functional analyses, recombinant and NHDF-derived POSTN significantly accelerated melanoma cell proliferation via the integrin/mitogen-activated protein kinase (MAPK) signaling pathway in vitro. The size of implanted melanoma tumors was significantly suppressed in *POSTN/Rag2* double knockout mice compared with *Rag2* knock-out mice. These results indicate that NHDF-derived POSTN accelerates melanoma progression and might be a promising therapeutic target for malignant melanoma.

Significance

In this study, we found an extracellular matrix protein, periostin (POSTN), increased in invasive melanoma compared with radial growth melanoma a quantitative proteomics approach, the 'isobaric tags for relative and absolute quantitation (iTRAQ)' method. POSTN was exclusively expressed in the tumor-associated stromal tissue not in the tumor cells, suggesting the paracrine effect of POSTN to melanoma cells aggressiveness. As expected, secreted POSTN could augment cell proliferation in melanoma cell lines in vitro. Moreover, we generated of *postn* and *rag2* double knockout mice and showed significant inhibition of human melanoma growth in those *KO* mice in vivo. This study could give us the cue of therapeutic effect on melanoma growth by an agent controlling tumor microenvironment induced by POSTN.

Introduction

Malignant melanoma is one of the most aggressive malignancies due to its strong capacity to grow, invade and metastasize, and therefore, it is of high priority to identify novel therapeutic targets and treatment options for this cancer.

Periostin (POSTN), first described in 1993 in mouse osteoblasts as osteoblast-specific factor 2 (OSF-2), is a secreted matrix N-glycoprotein of 93 kDa (Takeshita et al., 1993). The N-terminal region contains four fasciclin-like domains as well as several glycosylation sites. The protein originally was identified in MC3T3-E1 osteoblast-like cells, where it promotes integrin-dependent cell adhesion and motility. It shares homology with the insect cell adhesion molecule fasciclin I, with human β IgH3, and is induced by transforming growth factor-β (TGF-β) (Horiuchi et al., 1999), bone morphogenic protein-2 (Inai et al., 2008), IL-4, IL-13 (Takayama et al., 2006), and PDGF-bb (Li et al., 2006). As a ligand to alpha(V)beta(3) and alpha(V)beta(5) integrins, POSTN appears to activate the Akt/PKB (protein kinase B) pathway, which is known to facilitate cell survival and tumorigenesis (Bao et al., 2004; Gillan et al., 2002; Yan and Shao, 2006).

POSTN promotes the epithelial–mesenchymal transition (EMT), cancer cell growth, angiogenesis, invasiveness, and metastasis in several cancers (Bao et al., 2004; Baril et al., 2007; Erkan et al., 2007; Gillan et al., 2002; Kudo et al., 2006; Li et al., 2002; Puppin et al., 2008; Riener et al., 2010; Sasaki et al., 2001, 2002, 2003; Shao et al., 2004; Soltermann et al., 2008a,b; Tilman et al., 2007; Tischler et al., 2010). Although it was also reported that melanomas expressed POSTN (Tilman et al., 2007), the precise roles and the source of POSTN in malignant melanoma are still unclear.

We investigated the functional role of POSTN during melanoma tumor progression in vitro *and* in vivo. Moreover, we herein demonstrate that stromal cells, normal human dermal fibroblasts (NHDFs), were important sources of POSTN in cutaneous malignant melanoma and that NHDFs promote tumor growth and progression and modulate the tumor microenvironment by secreting POSTN in cutaneous malignant melanoma.

Results

Protein expression profiles in melanoma and normal skin

To identify the proteins associated with the progression of melanoma, we performed comparative protein expression profiling between in situ melanoma tissues and matched normal skin tissue, or between invasive melanoma tissue and matched normal skin tissues. We identified a total of 1062 proteins, and 1036 proteins were quantitatively analyzed by the iTRAQ 4-plex technology using a nano LC-MS/MS analysis. The complete list of all proteins identified is shown in Table S1. Among the identified proteins present at different levels in the invasive melanoma lesions compared with matched normal skin, 30 proteins were found to have increased more than 15-fold, while 67 proteins decreased to <0.25-fold (Table S1). As expected, S100, a protein previously known to be overexpressed in melanoma, was identified as one of the overexpressed proteins. Interestingly, POSTN was found to have a 25.703-fold higher expression in invasive tumor tissue compared with matched normal skin and showed a 4.434-fold higher expression in in situ tissue compared with matched normal skin (Table S1).

Expression of POSTN in melanomas

To confirm the altered expression of POSTN in invasive melanoma, we performed a Western blot analysis using proteins extracted from the same samples. As shown in Figure 1, POSTN was highly expressed in invasive melanoma tissue and slightly expressed in in situ tissue, although POSTN was faint in normal skin tissue (Figure 1A).

We thereafter preformed an immunohistochemical analysis of 20 invasive melanoma tissues and five metastatic lymph nodes. The expression of POSTN was observed in all invasive melanoma tissue samples and metastatic lymph nodes (Figure 1B). POSTN was localized in the stroma of the invasive melanoma, with a mesh-like structure (Figure 1C). Together, these data demonstrate that POSTN was overexpressed in invasive melanoma at the protein level; this was consistent with the results of our iTRAQ analysis.

POSTN is produced by NHDF instead of melanoma cells

We also analyzed the expression of POSTN in the cell lysates from three melanoma cell lines (MeWo, G-361, and VMRC-MELG) and melanocytes by Western blot analysis; however, the expression of POSTN was not observed in these cells (Figure 2A). Because POSTN was expressed in melanoma tissue samples, but not in melanoma cell lines, we hypothesized that an interaction between melanoma cells and NHDFs was required for the optimum expression of POSTN. First, we cocultured NHDFs with the MeWo, G-361, and VMRC-MELG cell lines and performed RT-PCR and a Western blot analysis. An overexpression of POSTN mRNA was only observed in the cocultured cell lysates (Figure 2B), and POSTN protein was detected in the cocultured supernatant in a time-dependent manner (Figure 2C).

To identify the source of POSTN, we cocultured NHDFs with CFSE-labeled MeWo cells for 48 h, and sorted these cells into NHDF and MeWo populations. The expression of POSTN mRNA measured by RT-PCR showed the source of the POSTN to be the NHDFs, not the MeWo cells (Figure 2D).

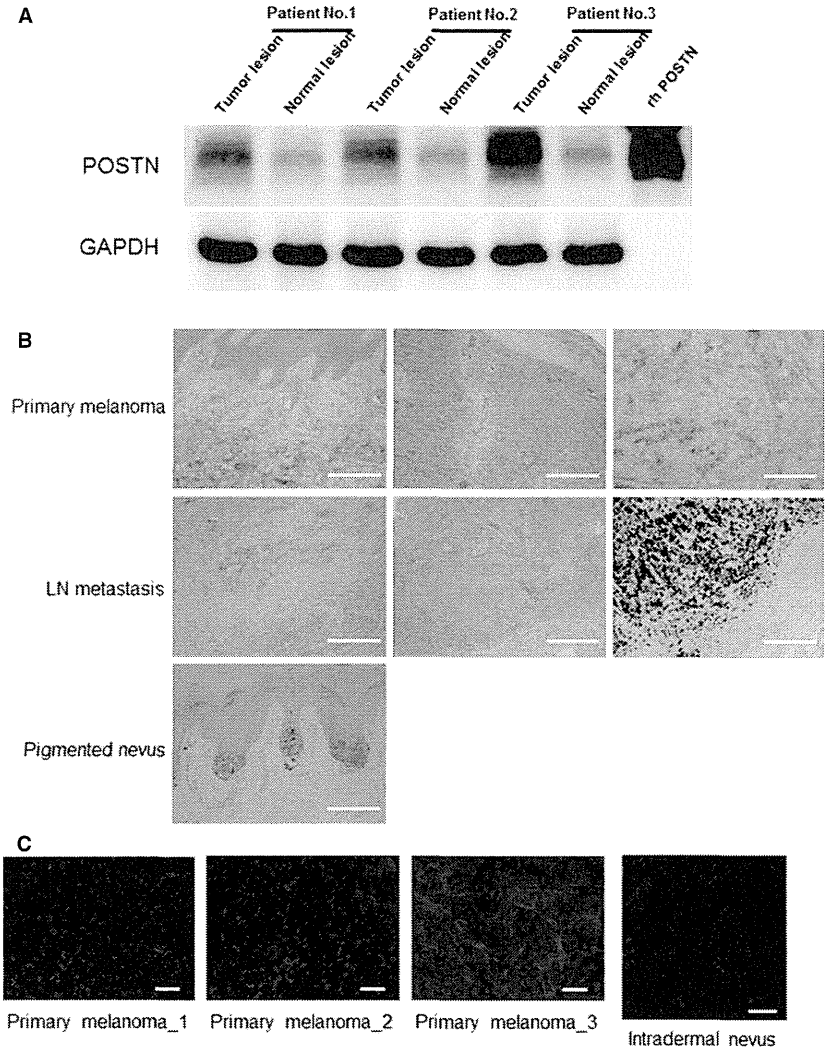

Figure 1. POSTN expression is much higher in melanoma tumor tissues compared with normal lesions. POSTN is predominantly expressed in the stroma of the melanoma tumors not melanoma cells. POSTN was slightly expressed in the in situ melanoma tissues (patient No. 1, No. 2) and highly expressed in the invasive melanoma tissues (patient No. 3) in a Western blot analysis (A). POSTN staining of invasive melanoma samples (upper three panels) and metastatic lymph nodes (*middle three panels*), but no expression of POSTN was detected in the pigmented nevus (lower left panel). Positive cells are stained red with ALP colorization. Bar indicates 100 μm (B). The confocal microscopic analysis showed that POSTN was strongly expressed in the stromal tissue with a lattice pattern in the 3 melanoma tissues (left 3 panels) not in the intradermal nevus (right panel). Bar indicates 20 μm for melanoma and 10 μm for intradermal nevus, respectively (C).

TGF-β1 and TGF-β3 mRNA expression in NHDFs after the coculture with melanoma cells

While the coculture of NHDF and melanoma cells was effective for the induction of POSTN expression, it was unclear how POSTN was induced during the coculture. To investigate the effect of soluble factors secreted by melanoma cells, we cultured NHDFs in the conditioned medium from MeWo or G-361 cells, and measured the expression of POSTN. However, the overexpression of POSTN was not observed at the protein level during these experiments (Figure 2E).

Next, to detect the soluble factors inducing POSTN in NHDFs, we examined the expression of POSTN-inducing cytokines, such as TGF-β1, 3, IL-4, IL-13, BMP2, and PDGF-bb, which are known to be soluble inducers of POSTN. During the RT-PCR analysis, IL-4, IL-13, BMP2, and PDGF-bb mRNA were not affected after the cocultured of melanoma cells and NHDFs (Figure 2F). However, TGF-β1 and TGF-β3 mRNA were both significantly upregulated in the cocultured NHDFs (Figure 2F). In addition, neutralization of TGF-β in the coculture markedly blocked the increase in POSTN expression (Figure 2G).

These findings indicate that cell–cell contact between NHDFs and melanoma cells is important for the expression of TGF-βs and POSTN from NHDFs, but the secretion of proteins from melanoma cells is not important for this effect.

Expression of integrin αvβ3 and αvβ5 in melanoma cells

Because integrin αvβ3, αvβ5, and α6β4 are well-known receptors for POSTN, we investigated the expression of these molecules by a Western blot analysis. We observed the expression of integrin αvβ3 and αvβ5 in the MeWo and G-361 cell lines (Figure 3A). On the other hand, integrin α6β4 was not expressed in the melanoma cells (data not shown).

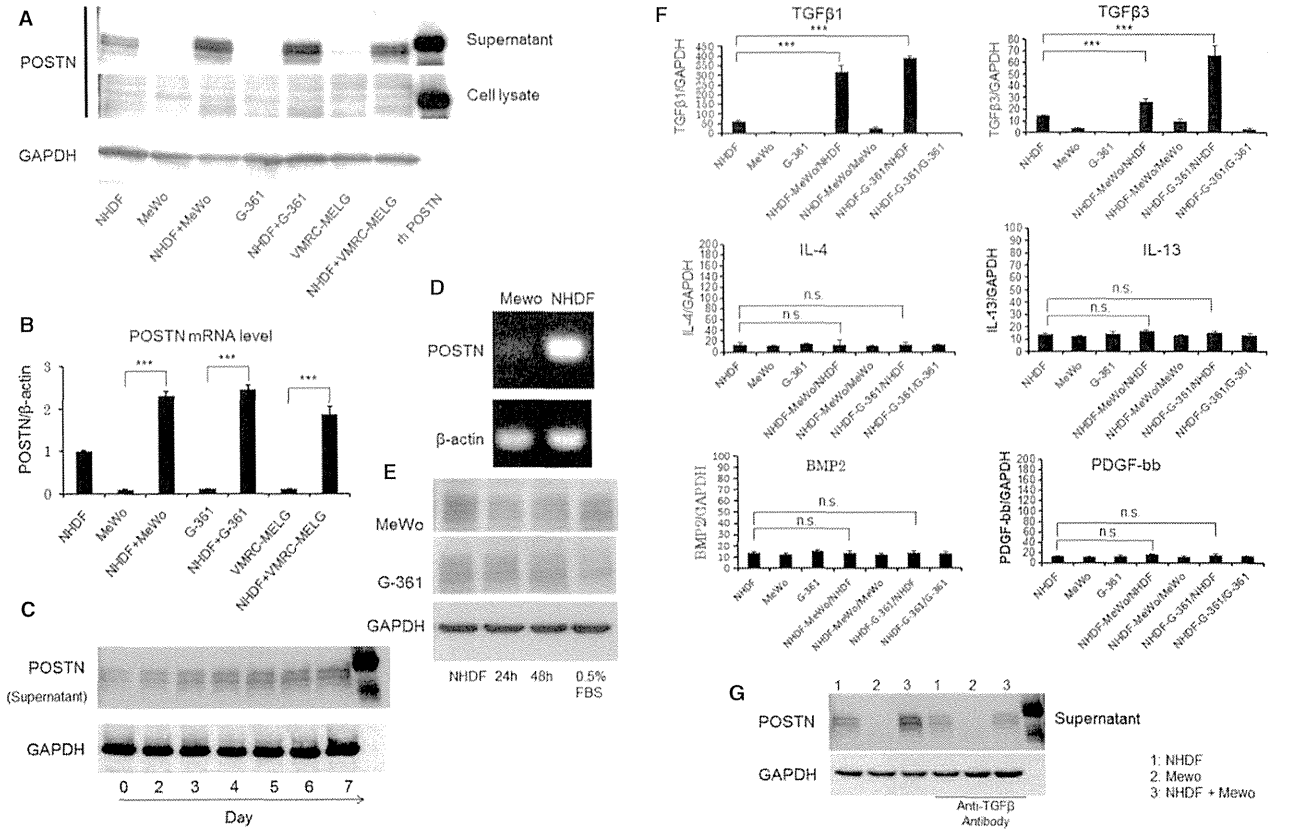

Figure 2. NHDFs secret POSTN during the coculture with human melanoma cells. The POSTN protein was upregulated in the supernatant after the coculture of NHDFs with human melanoma cells as determined by a Western blot analysis (A). POSTN mRNA was upregulated in the cell lysates after the coculture of NHDFs with human melanoma cells (B). POSTN expression was upregulated in the coculture media in a time-dependent manner (C). NHDFs, but not MeWo cells, induced POSTN expression under the coculture conditions (D). POSTN was not upregulated in the treatment with the conditioned media (E). The levels of TGFβ1, TGFβ3, IL-4, IL-13, BMP2, and PDGF-bb from NHDFs were increased after the coculture of NHDFs with melanoma cells (F). POSTN expressions were evaluated in cultured cells with or without anti-TGF-β neutralizing antibody (10 μg/ml, #MAB1835, R&D system, Minneapolis, MN). Neutralization of TGF-β blocked the increase in POSTN periostin in cocultured NHDF (G). *** indicate P-value <0.001.

Recombinant POSTN protein accelerates the proliferation of melanoma cells

To investigate the role of POSTN in the proliferation of human melanoma, we performed the MTT proliferation assay using recombinant human POSTN. The melanoma cells proliferated significantly more than control cells following the treatment with recombinant POSTN (Figure 3B). The proliferation in response to the treatment with recombinant POSTN was suppressed by anti-integrin $\alpha v\beta 3$ and $\alpha v\beta 5$ antibodies, which can neutralize the stimulation by POSTN (Figure 3C).

The phosphorylation of Akt and p44/42MAPK was observed in the cells treated with 100 ng/ml of recombinant POSTN (Figure 3D). However, the proliferation in response to the treatment with recombinant POSTN was abrogated by treatment with a MAPK inhibitor (PD98095), but not with an Akt inhibitor (LY294002) (Figure 3E). These results indicate that POSTN promotes melanoma proliferation *via* the integrin/p44/42MAPK pathway.

NHDF-derived POSTN gene transfection promotes the proliferation of melanoma cells

To investigate the role of NHDF-derived POSTN in melanoma, we transfected the NHDF-derived POSTN gene into MeWo cells (POSTN-low: lower POSTN expressing MeWo cells, POST-high: higher POSTN expressing MeWo cells, Figure 4A) and performed the MTT proliferation assay. The proliferation of POSTN–MeWo cells was significantly upregulated compared with control–MeWo (CTL-MeWo) cells in a time-dependent manner and much higher in POSTN-high cells (Figure 4B).

Significant suppression of human melanoma tumor growth in *POSTN* gene-deficient mice

We established immunodeficient Rag2 knockout mice (*Rag2* KO mice) and POSTN and Rag2 double knockout mice (*POSTN/Rag2* KO mice). We transplanted the MeWo human melanoma cell line subcutaneously onto the back of each of 17 mice and measured the tumor size for 70 days. The resulting tumors were smaller in the

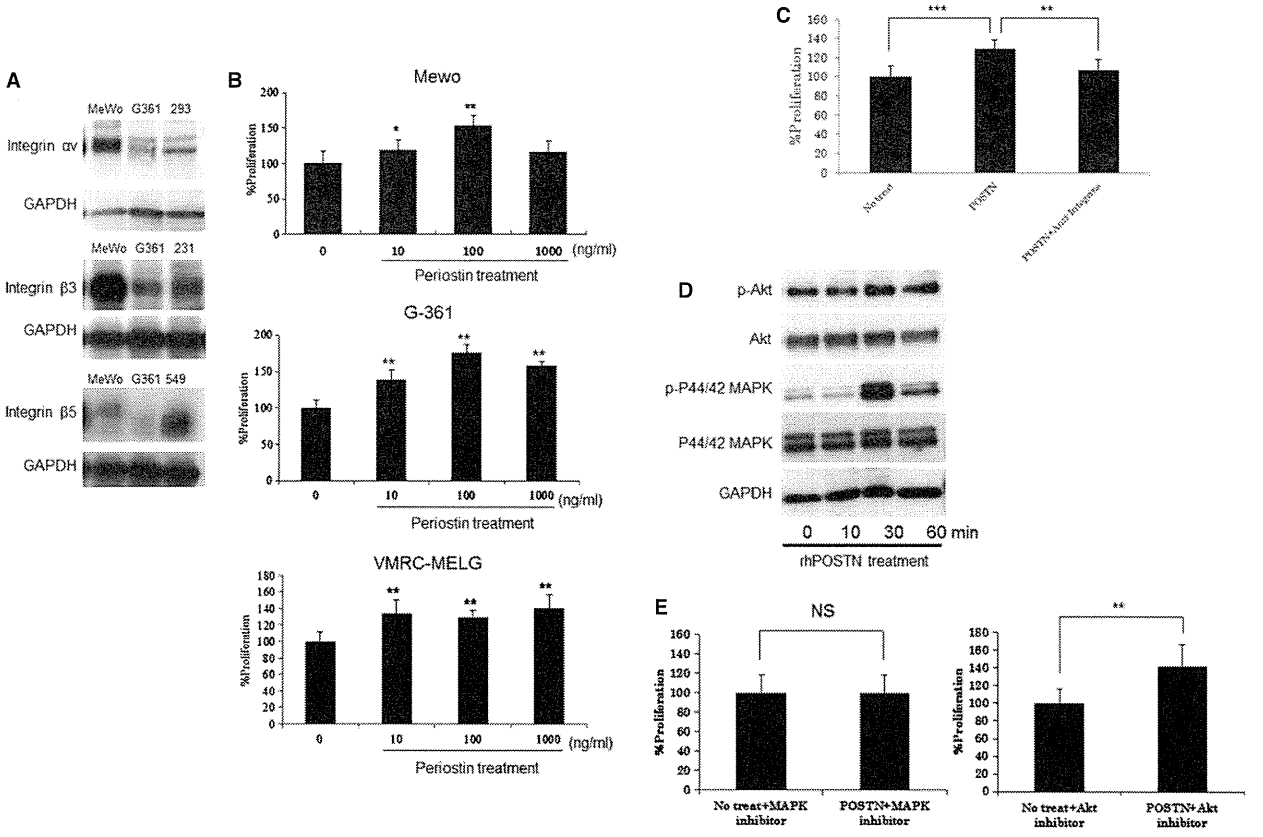

Figure 3. Recombinant POSTN protein accelerates melanoma cell proliferation via the integrin/P44/42MAPK pathway. Integrins αv, β3, and β5 were expressed in human melanoma cell lines (A). Recombinant POSTN increased the proliferation of human melanoma cells (MeWo, G-361, VMRC-MELG) (B). Neutralization of integrins αvβ3 and αvβ5 inhibited MeWo proliferation after the treatment with recombinant POSTN (C). The phosphorylation of Akt and P44/42MAPK in MeWo cells after the indicated treatment (D). Significant inhibition of MeWo cell proliferation after the treatment with recombinant POSTN by MAPK or Akt inhibitor (E). *, **, and *** indicate P-value <0.05, <0.01, <0.001, respectively.

double KO mice on day 56 after transplantation compared with the single KO mice (Figure 5A). The number of Ki-67-positive cells was significantly lower in the double KO mice compared with *Rag2* KO mice which indicated decrease in cell proliferation (Figure 5B, C). The levels of the αSMA protein, known as a marker of myofibroblasts and collagen tissue, which is colored red with E-V (Elastica van Gieson) staining, were decreased (Figure 5B). The growth of implanted melanoma tumors was also significantly suppressed in the double KO mice (Figure 5D).

Discussion

In this study, we reported the expression and function of POSTN in the ontogeny and progression of human malignant melanoma. We first noted the upregulation of POSTN protein expression in melanoma tissues compared with adjacent normal skin using an iTRAQ analysis, thereafter confirmed that higher expression in invasive melanoma. These results suggested that the upregulation of POSTN expression might be associated with the tumor malignancy. In the confocal microscopic analysis, POSTN was predominantly found to be distinctively localized in the stroma of invasive melanoma tissue, but not in cultured melanoma cells, thus suggesting the possibility that POSTN is derived from NHDFs to affect the melanoma microenvironment. The coculture of human melanoma cells with NHDFs robustly induced POSTN expression. These results indicate that POSTN expression is produced by NHDFs, but not by melanoma cells.

Recent studies have revealed that interactions between tumor cells and the surrounding stroma play an important role in facilitating tumor growth and invasion. In the present study, the induction of TGF-β in NHDF was found by melanoma cell–NHDF cell contact, and the behavior of dermal fibroblasts was altered to promote tumor growth and invasion by the interaction with surrounding melanoma cells. As reported previously, integrin was found to activate autocrine TGF-β signaling (Asano Y et al., 2005). In the present study, integrin was found highly expressed in melanoma cells (Figure 3). It suggested the similar mechanism of activated autocrine TGF-β signaling by integrin might be involved in the interaction of melanoma cell–NHDF.

Recent studies have revealed the importance of the fibrotic microenvironments surrounding cancer cells and the interactions between the host tissue and cancer cells

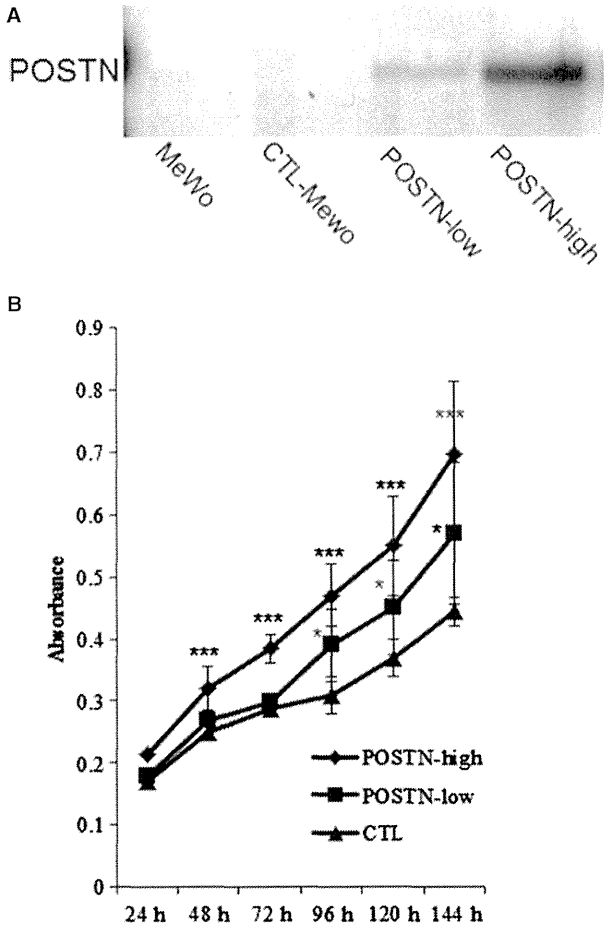

Figure 4. There is a significant increase in the proliferation of *POSTN*-transfected MeWo cells. *POSTN* gene transfection into MeWo cells (A). *POSTN* gene transfection upregulates the proliferation of MeWo cells (B). * and *** indicate P-value <0.05, <0.001, respectively.

for tumor growth and progression, because tumors are dependent on the normal host tissue-derived stromal cells and vasculature for growth and sustenance (Hanahan and Weinberg, 2000; Nyberg et al., 2008; Polyak and Kalluri, 2010; Quaranta, 2002; Yang et al., 2003; Zeisberg et al., 2002). Although there has been no previous report of a role of POSTN as stromal microenvironment in malignant melanoma, our data suggest that such a role exists.

We previously reported that POSTN accelerates dermal fibroblast proliferation, migration (Ontsuka et al., 2012), and myofibroblast differentiation, collagen 1 production (Yang et al., 2012), resulting in dermal fibrosis, and Elliott et al. also revealed the modulation of myofibroblast differentiation by POSTN (Elliott et al., 2012). These data support that NHDF-derived POSTN overexpression in the stroma of melanoma could affect the stromal microenvironment by activating dermal fibroblasts followed by tumor progression. In another report, impaired fibrous capsule formation of the implanted tumor was found in *periostin*-null mice, resulting in accelerating the tumor expansion (Guarino, 2010). Although our present data seem to be opposite of the previous report, MeWo cell established from human melanoma did not histologically form the surrounding fibrous capsule and the tumor immunity was canceled on the basis of Rag2 KO immune-deficient mice. Periostin expressed on intertumor space may be affected to accelerate adjacent melanoma cells in the present study setting.

We also revealed the proliferative effect of POSTN in human melanoma using recombinant and NHDF-derived POSTN. In details, we investigated the phosphorylation of FAK, STAT3, Akt, and p44/42MAPK, which are known to be the downstream pathways of integrin signals (Guarino, 2010). We did not observe any increase in the phosphorylation of FAK or STAT3 (data not shown), but upregulated phosphorylation of Akt and p44/42MAPK was observed after the treatment with recombinant POSTN. We also revealed that the proliferative effect of POSTN in melanoma is mediated by the integrins $\alpha v\beta 3$ and $\alpha v\beta 5$/p44/42MAPK signaling pathway, but not by the Akt pathway which is previously reported pathway (Bao et al., 2004; Ouyang et al., 2009; Yang et al., 2012).

To investigate the agonistic effect of POSTN on melanoma tissue growth in vivo, we transplanted MeWo cells into Rag2 KO mice and POSTN/Rag2 KO mice. The number of cells that were positive for Ki-67 was significantly decreased in the tumors of POSTN KO mice. In addition, the number of αSMA positive cells and the collagen expression which are known to be induced by POSTN in our previous study (Yang et al., 2012) were also decreased in POSTN KO melanomas, thus suggesting that there was suppression of the stromal microenvironment in these melanomas.

It has been reported that the POSTN expression in several cancers plays important roles in cancer progression as a result of increased proliferation, migration (Gillan et al., 2002), EMT (Soltermann et al., 2008a,b), and angiogenesis (Shao et al., 2004). In this study, our findings showed the source of POSTN to be restricted to NHDFs in human melanoma tissues, and that these stromal NHDFs between tumor cells may activate melanoma cell progression and invasion through an enhanced deposition of POSTN in the melanoma microenvironment.

Recent advances in the therapeutic approach for advanced melanoma have led to many clinical trials for patients with melanoma. For example, a BRAF inhibitor was reported to dramatically improve the prognosis of patients with melanoma. However, it was only effective in patients with the *V600E* gene mutation in the tyrosine kinase site (Atefi et al., 2011; Flaherty et al., 2010). Treatment with an anti-CTLA4 antibody can augment the anti-tumor immune response against melanoma tissue by blocking the immune-attenuating molecule, CTLA4, in T cells. However, the administration of the CTLA4 antagonist can induce severe autoimmune reactions, such as colitis and skin rashes (Weber, 2008). Therefore, it is essential to look for other therapeutic modalities with

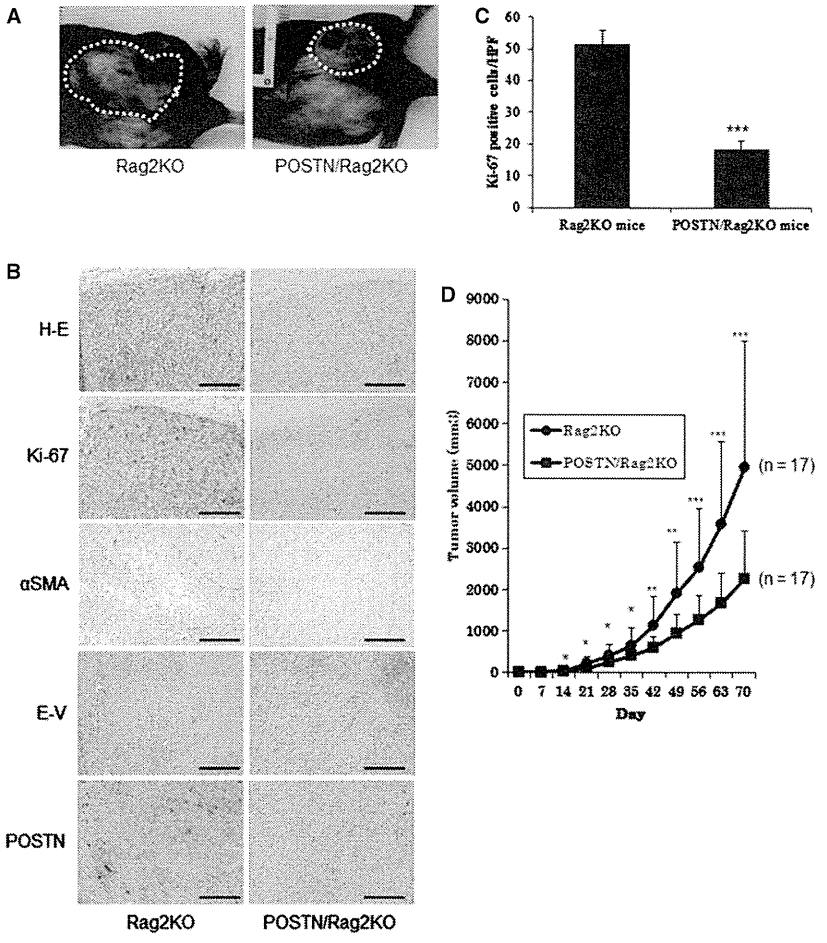

Figure 5. Melanoma tumorigenesis is significantly suppressed in *POSTN* gene knockout mice. Macroscopic feature of the *Rag2* KO and *POSTN/Rag2* KO mice on the day 56 after human melanoma cell implantation (A). There was decreased expression of Ki-67, αSMA, and collagen in the tumors of *POSTN/Rag2* KO mice. Dermal myofibroblast is positive for αSMA staining and collagen tissue becomes red by E-V (Elastica van Gieson) staining. Bar indicates 250 μm (B). There was a significant decrease in the number of Ki-67-positive cells in *POSTN/Rag2* KO mice (C). There was significant suppression of melanoma tumorigenesis in *POSTN* gene knockout mice (D). *, **, and *** indicate P-value <0.05, <0.01, <0.001, respectively.

novel mechanism(s) of action, which are not associated with such life-threatening adverse events. We believe that POSTN is important for the growth of melanoma, because the implanted melanoma cell grew more slowly in *POSTN*-depleted mice compared with matched control mice. A therapeutic approach targeting POSTN and its related signaling may lead to a safer treatment for malignant melanoma, and one that is less likely to be thwarted by resistance of the cancer cells.

In this experimental setting, there was no significant improvement in the overall survival in the POSTN-depleted mice even though the tumor growth was attenuated in KO mice compared with control mice on an immune-deficient background. There is no doubt that the survival is strongly dependent on the metastasis of the inoculated tumor cells, but we did not observe any metastasis in either the KO or wild-type mice, which likely contributed to the lack of a difference in the overall survival between the groups.

In conclusion, in human melanoma tissue, NHDFs interacted with melanoma cells to induce POSTN, which directly promoted melanoma cell proliferation by activating integrin/p44/42MAPK signals and indirectly instituted a fibrotic microenvironment in the tumor, thus resulting in a progression of the melanoma. As a result, the suppression of POSTN represents a novel therapeutic target for cutaneous malignant melanoma.

Methods

Cells and tissue samples

Human melanoma cell lines (MeWo, G-361, and VMRC-MELG) were obtained from the Japanese Collection of Research Bioresources (JCRB, Osaka, Japan), and NHDFs were obtained from TaKaRa Bio (Shiga, Japan). 293, 231, and A549 were represented by HEK293, MDA-MB-231, and A549 cancer cell lines loaded as positive controls, respectively (JCRB). All melanoma and normal tissue samples were obtained from patients at Osaka University Hospital (Department of Dermatology, Osaka, Japan). All clinical samples were collected after approval was obtained from the local ethics committee, and informed consent was obtained from each patient for use of the samples. Details of cell culture are described in Data S1.

Mice

Twelve-week-old Rag2-deficient (*Rag2*$^{-/-}$, C57BL/6 background) and periostin-deficient (*Postn*$^{-/-}$, C57BL/6 background) mice were used for the studies (Shimazaki et al., 2010). Experiments were undertaken following the guidelines for the care and use of experimental animals as required by the Japanese Association for Laboratory Animals Science (1987).

Sample preparation and iTRAQ labeling

Proteins were extracted from the frozen tumor and normal skin tissue samples. Details are described in Data S1.

Extracted proteins were purified using a 2D clean-up kit (GE Healthcare, Buckinghamshire, UK). Subsequently, 100 μg of each protein was dissolved, reduced, alkylated, and digested with trypsin, according to the manufacturer's protocol (Applied Biosystems, Foster City, CA, USA). The samples were labeled with iTRAQ reagent: reagent 114 for melanoma in situ, reagent 115 for normal skin lesions of melanoma in situ, reagent 116 for invasive melanoma, and reagent 117 for normal skin lesions of invasive melanoma. The labeled peptide samples were mixed and fractionated as described previously (Serada et al., 2010).

Mass spectrometric analysis and iTRAQ data analysis

NanoLC-MS/MS analyses and iTRAQ data analysis were performed as described in Data S1.

Western blot analysis

Cell lysates and supernatant fluids were used for the Western blot analyses. Details were described in Data S1.

Immunohistochemistry

Patient with paraffin-embedded melanoma tissue sections and in vivo mice melanoma tissue sections were stained with hematoxylin and eosin (H&E). For the immunohistochemical analysis, primary antibodies were used at the following dilutions: the human and mouse anti-POSTN (1:3000; Abcam, Tokyo, Japan), mouse anti-Ki-67 (1:500; Novocastra Laboratories Ltd, Newcastle, UK), and mouse anti-α-smooth muscle actin (α-SMA; 1:3000 dilution; Sigma-Aldrich, St. Louis, MO, USA). Details are described in Data S1.

Reverse transcription polymerase chain reaction (RT-PCR) analysis

To confirm the altered expression of POSTN in melanoma cells and NHDFs, melanoma cells (MeWo, G-361, and VMRC-MELG), NHDFs, and the cocultured cell samples were subjected to RT-PCR. β-actin was used as a housekeeping gene to evaluate and compare the quality of different cDNA samples. The primer sequences and the expected sizes of PCR products were as follows:

periostin, forward, 5′-TTGAGACGCTGGAAGGAAAT-3′

reverse, 5′-AGATCCGTGAAGGTGGTTTG-3′ (199 bp);

β-actin, forward, 5′-AGCCTCGCCTTTGCCGA-3′

reverse, 5′-CTGGTGCCTGGGGCG-3′(174 bp);

Details of total RNA extraction, quantitect reverse transcription, and RT-PCR are described in Data S1.

Quantitative reverse transcription polymerase chain reaction (qT-PCR) analysis

Normal human dermal fibroblasts were cocultured with CFSE-labeled MeWo and G-361 cells for 24 h. Thereafter, we sorted these cells into NHDF, MeWo, and G-361 cells using a FACS system. Next, the total RNA was isolated from the sorted NHDF, MeWo, and G-361 cells, and the products were reverse-transcribed into cDNA. The expression of TGFβ1, TGFβ3, IL-4, IL-13, BMP2, and PDGF-bb was measured using the Power SYBR Green PCR Master Mix (Applied Biosystems, Tokyo, Japan) according to the manufacturer's protocol. Glyceraldehyde-3-phosphate dehydrogenase (GAPDH) was used to normalize the mRNA, as GAPDH was not affected by the treatment. The primer sequences used were as follows:

TGFβ1, forward, 5′-TCGCCAGAGTGGTTATCTTTTG-3′

reverse, 5′-AGGAGCAGTGGGCGCTAAG-3′;

TGFβ3, forward, 5′-GCCCTTGCCCATACCTCCGC-3′

reverse, 5′-CGCAGCAAGGCGAGGCAGAT-3′;

GAPDH, forward, 5′-GGAGTCAACGGATTTGGTCGTA-3′

reverse, 5′-GCAACAATATCCACTTTACCAGAGTTAA-3′;

IL-4, forward, 5′-ACATTGTCACTGCAAATCGACACC-3′

reverse, 5′-TGTCTGTTACGGTCAACTCGGTGC-3′;

IL-13, forward, 5′-GCAATGGCAGCATGGTATGG-3′

reverse, 5′-AAGGAATTTTACCCCTCCCTAACC-3′;

BMP2, forward, 5′-ACTCGAAATTCCCCGTGACC-3′

reverse, 5′-CCACTTCCACCACGAATCCA-3′;

PDGF-bb, forward, 5′-CAGCGCCCATTTTTCATTCC-3′

reverse, 5′-GTTTTCTCTTTGCAGCGAGGC-3′.

Construction of a NHDF-derived POSTN expression vector

To construct a NHDF-derived POSTN expression vector, the cDNA of human POSTN derived from NHDFs cocultured with melanoma cells was amplified. The amplified cDNA was then inserted into the pcDNA3.1/V5-His-TOPO vector (Invitrogen, Carlsbad, CA, USA) and designated pcDNA3.1-POSTN.

Generation of NHDF-derived POSTN stable transfectant melanoma cells

To generate NHDF-derived POSTN stable transfectant cells (POSTN–MeWo), the MeWo cell line was transfected with pcDNA3.1-POSTN using Lipofectamine 2000 (Invitrogen) according to the manufacturer's instructions, after which the cells were selected with 500 μg/ml of Geneticin (GIBCO; Invitrogen). Stable clones were maintained in 250 μg/ml of Geneticin.

Proliferation assay

The proliferation of MeWo, G-361, VMRC-MELG, and POSTN–MeWo melanoma cells was examined using the Cell Counting Reagent SF (Nacalai Tesque, Kyoto, Japan) according to the manufacturer's recommendations, and then, absorbance was measured with a microplate reader (model 680; Bio-Rad, Tokyo, Japan) at test and reference wavelengths of 450 and 630 nm, respectively.

Kinase inhibition assays

The cells were incubated for 2 h with kinase inhibitors (Cell Signaling Technology, Beverly, MA, USA): LY294002 (10 μM) as an Akt inhibitor and PD98095 (10 μM) as a MAPK inhibitor. Cells were then stimulated with 100 ng/ml of recombinant POSTN in the same media. After stimulation, the MTT proliferation assay was performed.

Statistical analyses

The results are presented as the means + SD. The analyses were carried out using the two-sided, unpaired Student's *t* test or the two-sided Welch test. Multiple comparisons between groups were made by Fisher's or Dunnett's methods. We considered values to be significant when $P < 0.05$.

Acknowledgements

This study was supported by a Grant-in-Aid for Young Scientists (B) (22791100) from the Japanese Ministry of Education, Science, Sports, and Culture; a Grant-in-Aid for the Program for Promotion of Fundamental Studies in Health Sciences of the National Institute of Biomedical Innovation; and a Grant-in-Aid from the Ministry of Health, Labour, and Welfare of Japan.

Disclosure statement

All authors declare no financial support or relationship that may pose conflict of interest.

References

Asano Y, I.H., Yamane K, J.M., Mimura, Y., and Tamaki, K. (2005). Increased expression of integrin alpha(v)beta3 contributes to the establishment of autocrine TGF-beta signaling in scleroderma fibroblasts. J. Immunol. *175*, 7708–7718.

Atefi, M., von Euw, E., Attar, N. et al. (2011). Reversing melanoma cross-resistance to BRAF and MEK inhibitors by co-targeting the AKT/mTOR pathway. PLoS ONE *6*, e28973.

Bao, S., Ouyang, G., Bai, X. et al. (2004). Periostin potently promotes metastatic growth of colon cancer by augmenting cell survival via the Akt/PKB pathway. Cancer Cell *5*, 329–339.

Baril, P., Gangeswaran, R., Mahon, P.C. et al. (2007). Periostin promotes invasiveness and resistance of pancreatic cancer cells to hypoxia-induced cell death: role of the beta4 integrin and the PI3k pathway. Oncogene *26*, 2082–2094.

Elliott, C.G., Wang, J., Guo, X. et al. (2012). Periostin modulates myofibroblast differentiation during full-thickness cutaneous wound repair. J. Cell Sci. *125*, 121–132.

Erkan, M., Kleeff, J., Gorbachevski, A. et al. (2007). Periostin creates a tumor-supportive microenvironment in the pancreas by sustaining fibrogenic stellate cell activity. Gastroenterology *132*, 1447–1464.

Flaherty, K.T., Puzanov, I., Kim, K.B. et al. (2010). Inhibition of mutated, activated BRAF in metastatic melanoma. N. Engl. J. Med. *363*, 809–819.

Gillan, L., Matei, D., Fishman, D.A., Gerbin, C.S., Karlan, B.Y., and Chang, D.D. (2002). Periostin secreted by epithelial ovarian carcinoma is a ligand for alpha(V)beta(3) and alpha(V)beta(5) integrins and promotes cell motility. Cancer Res. *62*, 5358–5364.

Guarino, M. (2010). Src signaling in cancer invasion. J. Cell. Physiol. *223*, 14–26.

Hanahan, D., and Weinberg, R.A. (2000). The hallmarks of cancer. Cell *100*, 57–70.

Horiuchi, K., Amizuka, N., Takeshita, S. et al. (1999). Identification and characterization of a novel protein, periostin, with restricted expression to periosteum and periodontal ligament and increased expression by transforming growth factor beta. J. Bone Miner. Res. *14*, 1239–1249.

Inai, K., Norris, R.A., Hoffman, S., Markwald, R.R., and Sugi, Y. (2008). BMP-2 induces cell migration and periostin expression during atrioventricular valvulogenesis. Dev. Biol. *315*, 383–396.

Kudo, Y., Ogawa, I., Kitajima, S. et al. (2006). Periostin promotes invasion and anchorage-independent growth in the metastatic process of head and neck cancer. Cancer Res. *66*, 6928–6935.

Li, J.S., Sun, G.W., Wei, X.Y., and Tang, W.H. (2002). Expression of periostin and its clinicopathological relevance in gastric cancer. World J. Gastroenterol. *13*, 5261–5266.

Li, G., Oparil, S., Sanders, J.M. et al. (2006). Phosphatidylinositol-3-kinase signaling mediates vascular smooth muscle cell expression of periostin in vivo and in vitro. Atherosclerosis *188*, 292–300.

Nyberg, P., Salo, T., and Kalluri, R. (2008). Tumor microenvironment and angiogenesis. Front Biosci. *13*, 6537–6553.

Ontsuka, K., Kotobuki, Y., Shiraishi, H. et al. (2012). Periostin, a matricellular protein, accelerates cutaneous wound repair by activating dermal fibroblasts. Exp. Dermatol. *21*, 331–336.

Ouyang, G., Liu, M., Ruan, K., Song, G., Mao, Y., and Bao, S. (2009). Upregulated expression of periostin by hypoxia in non-small-cell lung cancer cells promotes cell survival via the Akt/PKB pathway. Cancer Lett. *281*, 213–219.

Polyak, K., and Kalluri, R. (2010). The role of the microenvironment in mammary gland development and cancer. Cold Spring Harb. Perspect. Biol. *2*, a003244.

Puppin, C., Fabbro, D., Dima, M. et al. (2008). High periostin expression correlates with aggressiveness in papillary thyroid carcinomas. J. Endocrinol. *197*, 401–408.

Quaranta, V. (2002). Motility cues in the tumor microenvironment. Differentiation *70*, 590–598.

Riener, M.O., Fritzsche, F.R., Soll, C. et al. (2010). Expression of the extracellular matrix protein periostin in liver tumours and bile duct carcinomas. Histopathology *56*, 600–606.

Sasaki, H., Dai, M., Auclair, D. et al. (2001). Serum level of the periostin, a homologue of an insect cell adhesion molecule, as a prognostic marker in nonsmall cell lung carcinomas. Cancer *92*, 843–848.

Sasaki, H., Sato, Y., Kondo, S. et al. (2002). Expression of the periostin mRNA level in neuroblastoma. J. Pediatr. Surg. *37*, 1293–1297.

Sasaki, H., Yu, C.Y., Dai, M. et al. (2003). Elevated serum periostin levels in patients with bone metastases from breast but not lung cancer. Breast Cancer Res. Treat. *77*, 245–252.

Serada, S., Fujimoto, M., Ogata, A. et al. (2010). iTRAQ-based proteomic identification of leucine-rich alpha-2 glycoprotein as a novel inflammatory biomarker in autoimmune diseases. Ann. Rheum. Dis. *69*, 770–774.

Shao, R., Bao, S., Bai, X. et al. (2004). Acquired expression of periostin by human breast cancers promotes tumor angiogenesis through up-regulation of vascular endothelial growth factor receptor 2 expression. Mol. Cell. Biol. *24*, 3992–4003.

Shimazaki, M., Nakamura, K., Kii, I. et al. (2010). Periostin is essential for cardiac healing after acute myocardial infarction. J. Exp. Med. *205*, 295–303.

Soltermann, A., Ossola, R., Kilgus-Hawelski, S. et al. (2008a). N-glycoprotein profiling of lung adenocarcinoma pleural effusions by shotgun proteomics. Cancer *114*, 124–133.

Soltermann, A., Tischler, V., Arbogast, S. et al. (2008b). Prognostic significance of epithelial-mesenchymal and mesenchymal-epithelial transition protein expression in non-small cell lung cancer. Clin. Cancer Res. *14*, 7430–7437.

Takayama, G., Arima, K., Kanaji, T. et al. (2006). Periostin: a novel component of subepithelial fibrosis of bronchial asthma downstream of IL-4 and IL-13 signals. J. Allergy Clin. Immunol. *118*, 98–104.

Takeshita, S., Kikuno, R., Tezuka, K., and Amann, E. (1993). Osteoblast-specific factor 2: cloning of a putative bone adhesion protein with homology with the insect protein fasciclin I. Biochem. J. *294*(Pt 1), 271–278.

Tilman, G., Mattiussi, M., Brasseur, F., van Baren, N., and Decottignies, A. (2007). Human periostin gene expression in normal tissues, tumors and melanoma: evidences for periostin production by both stromal and melanoma cells. Mol. Cancer. *6*, 80.

Tischler, V., Fritzsche, F.R., Wild, P.J. et al. (2010). Periostin is up-regulated in high grade and high stage prostate cancer. BMC Cancer *10*, 273.

Weber, J. (2008). Overcoming immunologic tolerance to melanoma: targeting CTLA-4 with ipilimumab (MDX-010). Oncologist *13*(Suppl 4), 16–25.

Yan, W., and Shao, R. (2006). Transduction of a mesenchyme-specific gene periostin into 293T cells induces cell invasive activity through epithelial-mesenchymal transformation. J. Biol. Chem. *281*, 19700–19708.

Yang, C., Zeisberg, M., Lively, J.C., Nyberg, P., Afdhal, N., and Kalluri, R. (2003). Integrin alpha1beta1 and alpha2beta1 are the key regulators of hepatocarcinoma cell invasion across the fibrotic matrix microenvironment. Cancer Res. *63*, 8312–8317.

Yang, L., Serada, S., Fujimoto, M. et al. (2012). Periostin facilitates skin sclerosis via PI3K/Akt dependent mechanism in a mouse model of scleroderma. PLoS ONE *7*, e41994.

Zeisberg, M., Maeshima, Y., Mosterman, B., and Kalluri, R. (2002). Renal fibrosis. Extracellular matrix microenvironment regulates migratory behavior of activated tubular epithelial cells. Am. J. Pathol. *160*, 2001–2008.

Supporting information

Additional Supporting Information may be found in the online version of this article:

Table S1. List of all proteins identified by iTraq.

Data S1. Methods.